Extracting Insights on Use of Force by Police in Encounters through Topological Data Analysis of Body-Worn Camera Video Datasets

Matthew Broussard* Bala Krishnamoorthy† David Makin‡ Dale Willits‡

August 8, 2018

Running head: Insights on Use of Force in Encounters through TDA of BWC Video Datasets

Address for correspondence: Bala Krishnamoorthy
VUB 347, Washington State University Vancouver
14204 NE Salmon Creek Ave, Vancouver, WA, 98686
Phone: (360) 546 9167

*Department of Mathematics and Statistics, Washington State University, Pullman, WA
†Department of Mathematics and Statistics, Washington State University, Vancouver, WA
‡Department of Criminal Justice and Criminology, Washington State University, Pullman, WA

Abstract

Objectives: This study introduces topological data analysis (TDA) for exploring complex datasets in criminology by exploring patterns of police use of force from annotated body-worn camera data on police interactions.

Methods: Data from 288 police-community interactions totaling over 33 hours of footage were annotated, including 70 incidents where officers used some level of force. TDA, making use of the Mapper algorithm and associated visualizations, is used to identify patterns, by race, gender and citizen behavior, of when and how police applied force during these interactions. The Mapper algorithm has the ability to identify subsets of the input dataset, i.e., subpopulations, that behave distinctly from the rest of the population. It simplifies high-dimensional data into visual forms that still reveal significant structural aspects, making this algorithm distinct from traditional data analysis techniques.

Results: The TDA models were stable over a range of parameter values and demonstrated how substantively meaningful patterns can be extracted from complex data. Our specific results suggest that there may be important configurations of gender, race, and behavior which help explain whether, when, and how police use force.

Conclusions: TDA provides researchers with a valuable tool that is subject to fewer assumptions and restrictions than many other approaches to help identify and visualize meaningful patterns within complex data. In the context of this study, our results highlight the need to study police-community interactions as complex processes and to be cautious of simplistic explanations for use of force behaviors.

Keywords: Use of force, body-worn camera videos, topological data analysis, Mapper.

1 Introduction

Police agencies are increasingly adopting Body-Worn Camera (BWC) programs. Though there are a variety of reasons for the adoption of BWC programs and BWC footage is used for a multitude of purposes, BWC footage has largely not been used as a systematic data source for research (for exceptions, see (Makin et al., 2018; Willits and Makin, 2018)). Yet, given the increased scrutiny of police agencies and the heightened levels of police-community tension (Wolfe and Nix, 2016), it is vitally important to understand how police-community interactions unfold. At the same time, police-community encounters can be complicated, emotional, and involve high stakes, and agencies often record hundreds, if not thousands, of hours of footage per day. Given that such datasets are quite complex, there is an increased need to employ sophisticated data analysis techniques to study police-community interactions. In particular, we are interested in gaining a detailed and nuanced understanding of the interplay of factors that together explain police officer and community member behavior during their interactions.

In this paper, we explore the use of techniques from topological data analysis (TDA) to extract insights from the detailed analysis of annotated BWC videos. TDA is an emerging subfield of mathematics that reveals the underlying structure of datasets at multiple scales, in ways not possible using traditional data analysis techniques (Lum et al., 2013). We do not present TDA as a replacement for regression analysis, one of the most widely used statistical

approaches in criminology and criminal justice, though we believe it is important to explore other potential computational approaches to data modeling. As Berk (2010) notes, while regression is a useful descriptive tool, there are a host of difficulties revolving regression analysis, statistical inference, and causality. Instead, we posit that visualization holds the key to the extraction of insights from complex datasets. Effective visual representations help overcome the shortcomings of relying purely on summary statistics to describe a dataset, as demonstrated by the famous example of Anscombe's Quartet (Anscombe, 1973). At the same time, it is typically hard to visualize high dimensional data, and can thus be difficult to characterize with meaningful patterns. Intuitively, TDA produces *low-dimensional visualizations* of high dimensional data under different lenses, revealing its complex structure in the process. The focus of our TDA approach is not on explaining the conditional distribution of an outcome variable, but on examining the multi-dimensional nature of data with the goal of identifying subgroups of interactions with police that show unique characteristics.

1.1 Studying Police-Community Interactions

Though TDA can be applied to virtually any type of quantitatively coded data, we focus here on its application to the study of police use of force. There is a broad literature on police use of force that has identified a number of important correlates. Researchers have examined the influence of gender, indicating police are more likely to use force against males (Terrill, 2005); race, suggesting African-American males are more likely to have forced used against them (Holmes and Smith, 2008) and that police are more likely to use force against non-white suspects (Gau et al., 2010); mental health, suggesting how the police interact with a person having a mental health issue may exacerbate the situation, influencing the odds for use of force (Morabito et al., 2012), as well as different sociodemographic characteristics, which were examined by a range of studies for the extent to which they influence the odds for use of force in a given situation. However, the resultant state of knowledge remains mixed, with recent research providing mixed results regarding the degree to which police are more likely to use lethal force against minorities (see (Cesario et al., 2018) and (Ross et al., 2018)), and other studies suggesting that race has limited to no influence over the odds that force is used in a given interaction (McCluskey et al., 2005; Morabito and Socia, 2015; Worrall et al., 2018)—offering instead that environmental and contextual factors explain the disproportionate rates of non-lethal use of force (Fryer, Jr, 2016; Jetelina et al., 2017).

Further, despite the importance of this work, researchers have questioned the quality of data available to study use of force. For example, Klinger (2012) has argued strongly against the use of the Supplementary Homicide Reports (SHR) for use in studying police use of force, both because the SHR data are limited to the narrow category of lethal force and because SHR estimates are often inaccurate. Moreover, Klinger and Brunson (2009) and Phillips (2018) argue that perceptual distortions affect police officers' ability to accurately recall details of incidents, suggesting that police incident narratives may be inaccurate in some instances and especially in more emotionally charged encounters. Lastly, Roussell et al. (2017) have argued that laboratory data on police use of force decisions should also be viewed with caution, as research has yet to demonstrate that decisions made in response to simulated scenarios can capture the emotionality that theorists have commonly linked to use of force decisions (Holmes and Smith, 2008).

We argue that data derived from BWCs constitute an important resource for studying police interactions in general and for use of force in particular. The proliferation of BWCs and continued advancement in this technology is in many ways a watershed moment in the study of police interactions. These cameras were employed, by and large, as a means of reasserting control over a narrative that was being established increasingly by a concerned public documenting police contacts via cell phone videos, and the rapid dissemination of such videos through social media platforms (Makin, 2016; Jennings et al., 2014; White, 2014). Although, as Nowacki and Willits (2016) suggest, progressive administrators and a robust technology infrastructure were dominant organizational predictors of whether an agency implemented a BWC program. Regardless of the impetus, the resultant integration represented a change in the equation of transparency and accountability concerning the practice of policing (Jackson, 2015), with large-scale adoptions by police agencies assuming these devices would reemphasize their commitment to transparency and accountability.

Because of this widespread and increasing adoption of BWCs, agencies generate hundreds and in some larger agencies, thousands, of hours of footage daily. Translating this footage into usable data is an arduous task, yet the systematic analysis of this footage presents extremely important data for documenting and understanding interpersonal interactions and factors associated with police and community decision-making (Makin et al., 2018; Willits and Makin, 2018). Indeed, prior to the availability of BWC data, police interactions were often studied through researchers' riding with officers and occasionally the use of systematic social observation (SSO) (Worden and McLean, 2014). Such work is undoubtedly important and yet inherently limited by the number of observations that could be collected, the reliance on notes and memory, participant selection effects, and potential researcher effects, such as the Hawthorne Effect. Conversely, the use of BWC footage addresses many of these issues by removing the researcher from the incident, by allowing for the examination of more encounters, and most importantly by providing a video and audio recording of what happened in an incident that can be watched and re-watched as necessary.

Still, such data and, in fact, the underlying circumstances surrounding police-citizen encounters are complex and difficult to study. Therefore, in addition to arguing for the use of BWC footage as recorded observational data, we also argue that the way police interactions are modeled and interpreted should take into account the various factors that influence the outcome of a given interaction. Traditionally, researchers have attempted to achieve this goal using regression analyses. When assumptions are met, regression analysis is a powerful tool for description, prediction, and inference. But in practice, there are often many problems with how regression is implemented by researchers (Berk, 2004). Under ideal conditions, regression analysis describes the conditional distribution of an outcome variable under given values for a set of independent or predictor variables. In this regard, regression analysis is excellent at the identification of key predictors for a given outcome variable. Yet, for complex social interactions, there is also value in identifying distinct subsets and patterns of outcomes. Regression analysis, while it can approximate such results through the inclusion of interactions and/or through subset analyses, is not designed to identify these types of results. This critique of regression research is not new. The work of Ragin (2014) on developing case-centric comparative methods is based on the premise that certain configurations of factors and variables produce outcomes and, indeed, that different combinations might produce the same outcome. The broad insight here is that while a predictor might have an average

conditional relationship with or effect on some outcome, the relationship between a particular independent variable and an outcome variable might depend greatly on the values of other variables for a specific case. Given the underlying complexity of police interactions and especially those that result in force, we demonstrate the utility and importance of identifying the nontrivial structure underlying such data sets using an approach distinct from regression analysis by studying use of force within encounters.

1.2 The Application of Topology to the Study of Police-Citizen Interactions

We posit that a topological approach to identify patterns of police interactions has great promise. Topological data analysis is a growing sub-field of mathematics based on the premise that all data, including higher dimensional data, have shape, and that analyzing the topological features of the shape of a given dataset can produce insights into the patterns and relationships within the data (Carlsson, 2009; Lum et al., 2013). Topology has many key properties that make extraction of patterns from large datasets highly effective. First, topology studies shapes in a coordinate-free way, which enables comparison among data sets derived from diverse sources or coordinate systems. In other words, as long as a notion of distance between data points is specified, the actual locations of the points is immaterial. Second, topological constructions are not sensitive to small changes in data and are robust against noise as these constructions are defined to be equivalent up to continuous deformations (e.g., a smooth circle and a wiggly circle are considered to be of the same topological "type"). This feature allows topological models to identify both small-scale and large-scale patterns in data. Third, topology works with highly compressed representations of spaces in the form of simplicial complexes, or triangulations (Munkres, 1984). These objects are higher order generalizations of graphs and preserve information relevant to how points in the dataset are connected. In fact, these representations result in drastic reductions in both the number of points as well as in the dimensions of the points. These representations sit in two or three dimensions usually, and consist of only a small number, e.g., around 20, of elements (nodes, edges, etc.).

Fourth, topological methods are far less restrictive in their assumptions on data than most statistical techniques. That is, rather than needing to test individually for specific types of distribution, these methods rely only on the sampled data being topologically well behaved. It has been shown that topological methods exhibit better sensitivity to both large- and small-scale patterns, compared to more traditional techniques such as principal component analysis, multidimensional scaling, manifold learning, and cluster analysis (Lum et al., 2013).

Finally, topological approaches lend themselves to visualization methods to display the complex structure of data. Police-community encounters and thus the BWC data associated with these encounters have complex structures. We posit that visualization holds the key to the extraction of insights from such complex datasets. The TDA pipeline we employ, called the *Mapper algorithm* (Singh et al., 2007), is designed to produce insightful visualizations of complex high-dimensional data sets under various lenses and at multiple scales. Starting with high-dimensional data, the Mapper algorithm creates representative structures in two

or three dimensions that capture important underlying structure of the original data, while being amenable to human interpretation.

2 Methods

2.1 Data

Data for this research were drawn from the annotation of 288 BWC videos from a single police agency, including 70 incidents in which there was use of force. This dataset represent all use of force incidents from this agency from 2013 to 2016, and a random sample of 218 criminal complaint incidents not involving force within the same time period. The videos used in this analysis amounted to well over 2000 minutes of double-coded footage. Given the sensitive nature of this data, IRB approval was secured to code and analyze the same. Each annotated interaction represents an incident involving a criminal complaint. Criminal complaints range from misdemeanor to felony crimes, and are acquired from a police agency that has fewer than 100 officers serving a small community (under 100,000 residents). Officers within the agency are primarily white and male with a range of years of service from less than one year to over 20 years of service.

Recognizing the complexity of converting BWC footage to objective data, we apply the principles of event modeling (Macnamara, 2005) through the demarcation of events within the interaction. For the purposes of this study, we focus on key events associated with the use of force. We create objective markers associated with each use of force. Subsequently, we can model each different use of force within the interaction, in addition to relevant contextual information. Therefore, each event becomes an objective marker within the video (thus an annotation), facilitating detailed quantitative analysis.

We use the annotation method described by Makin et al. (2018), which employs a three-tiered annotating process for BWC footage. This process allows the multi-stage verification of each annotated event, ensuring each annotation is accurately identified within the BWC footage. Specific to use of force, we annotate a Time-to-Force (TtF) variable calculated as the duration of time from the first point of contact to when force is used; the Duration-of-Force (DoF) calculated as the duration of time force is applied to the suspect and the suspect is fully restrained; and lastly, we calculate the level of force used within the interaction. For the purposes of this research, we replicate the categorical levels used by Willits and Makin (2018): 0 = no force used, 1 = minor force (verbal threats and pat downs), 2 = medium force (grappling with a suspect to maintain control), 3 = high force (the use of strikes and grappling resulting in impact), and 4 = instrument-based force (including chemical agents and police batons, as well as bean bag rounds). Table 1 presents the descriptive statistics associated with our key variables.

2.2 Analytic Approach

We use the *Mapper algorithm* as our topological data analysis tool to study police use of force. Originally proposed by Singh et al. (2007), the Mapper algorithm (also referred to simply as Mapper) has been used in a growing number of applications from diverse domains recently,

Table 1: Descriptive Statistics of main variables in our BWC video dataset. The second column lists the mean (average) value of the variable and its standard deviation when it is continuous, or the count of videos with value 1 when it is binary.

Variable	Mean (SD) or #	Description
Dependent Variables		
Use of Force	0.24, 70 Y	0 = NO, 1 = Yes (Y)
Uses of Force	0.87 (2.0)	Number of distinct times force is used
Time to Force	172.44 (270.71)	Seconds from officer identifying self to first use of force
Duration of Force	134.66 (138.74)	Maximum force used: 0–4, increasing severity
Suspect Characteristics		
Gender	210 M	0 = Female, 1 = Male (M)
Black	29 B	0 = Non-black, 1 = Black (B)
White	214 W	0 = Non-white, 1 = White (W)
Other	45 O	0 = Black/White, 1 = Other (O)
Aggression	1.31 (0.55)	1 = Low, 2 = Medium, 3 = High

ranging from medicine (Hinks et al., 2015; Li et al., 2015; Nicolau et al., 2011; Nielson et al., 2015; Rucco et al., 2015; Sarikonda et al., 2014; Torres et al., 2016) to agricultural biotechnology (Kamruzzaman et al., 2017) to basketball player profiles (Alagappan, 2012) to voting patterns (Lum et al., 2013). The key to all these success stories is the ability of Mapper to identify subsets of the input dataset, i.e., subpopulations, that behave distinctly from the rest of the data or population. In fact, this feature of Mapper distinguishes it from many traditional data analysis techniques based on, e.g., machine learning, where the goal is usually to identify predictive patterns valid for the entire data set.

Here, we employ the Mapper algorithm to extract patterns and identify subgroups related to police use of force that standard statistical analysis cannot detect. The Mapper algorithm simplifies high-dimensional data into visual forms that still reveal significant structural aspects. It takes as input a collection of data points X typically in some high-dimensional space ($\mathbb{R}^d$ for large dimension d). The second component is a *filter* function $f : X \to Z \subset \mathbb{R}$, defined on the points in X. More generally, the filter function could be high-dimensional, i.e., $f : X \to \mathbb{R}^h$ for some $h \geq 2$. Associated with the filter function is a decomposition of its range of values Z into a set of overlapping intervals, which is referred to as a *cover* of Z. The cover is characterized typically by the number of intervals n and an overlap percentage p, which are referred to as the *resolution* and *gain* of the cover, respectively. The resolution n determines the length of each interval (the intervals are assumed to be of the same length by default). The gain p determines by how much adjacent intervals in the cover overlap.

The main idea of the Mapper is to *pull back* the cover of Z to a cover of X, the input data set. In other words, for each interval in the cover of Z, the algorithm identifies subsets of points from X that have values of the filter function f in that interval. These points all have "similar" f values, and are grouped further into clusters by Mapper using a *distance function*. This clustering step is designed to reveal the covariance of, or relation between,

the filter function f and one or more other variables of interest that are used to define the distance function. Note that the clustering step is repeated for every interval in the cover of Z. Each cluster produced in this step is represented by a single vertex, or node, in the final object or representation—also called the *Mapper*.

Given that the intervals in the cover of Z overlap (as defined by the gain parameter p), clusters resulting from overlapping intervals of the cover could share data points. Such overlaps of membership between two clusters is represented by drawing an edge between the corresponding two nodes in the final object (and a triangle between three clusters that intersect, a tetrahedron between four intersecting clusters, and so on). These connections between clusters (as specified by the edges between the corresponding nodes) capture the covariation of f with other functions of interest across the range of values of the filter function.

Note that such covariations could be *nonlinear*, e.g., there could be two distinct paths of edges connecting disjoint series of clusters as one moves along a set of intervals in the cover of Z. Such disjoint paths capture subpopulations (i.e., subsets of points of X) displaying distinct behavior under "similar" conditions as captured by similar ranges of values of f. Of course, the distinct behavior would be explained by one or more of the other variables specified in the dataset X. Indeed, the key strength of the Mapper algorithm is its natural ability to identify such nontrivial "structure" while also capturing more straightforward linear relationships—all in a unified framework.

2.2.1 Illustration of the Mapper Algorithm

We illustrate the Mapper algorithm on a simple data set of points X in 2D, which appear to be sampled from a noisy circle. We use the height of the points (i.e., their y-coordinate values) as a filter function. Figure 1 shows the set X of points along with their "projection" on to the height axis (i.e., y-axis). Naturally, if we view the points just in this projection, we do not see the circular structure of the data set.

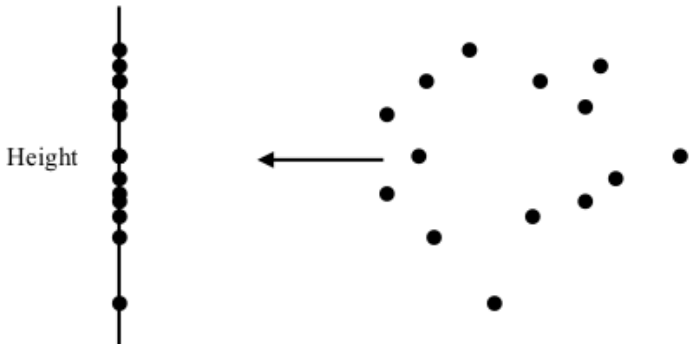

Figure 1: A data set of points in 2D, possibly sampled from a circle along with added noise.

Once a filter function f is chosen (height of the points here), the Mapper algorithm creates a cover for the range of f using n intervals $I_1, I_2, ..., I_n$ all of the same length, where each interval overlaps with its immediate neighbors by exactly p percent. The algorithm then takes the preimage under f of I_1, i.e., it identifies the points in X whose f values fall in I_1. This set of points, denoted $f^{-1}(I_1)$, is divided into clusters using a chosen clustering

algorithm. This step partitions the points in $f^{-1}(I_1)$ into one or more clusters, each of which is represented by a node in the final object or visualization. In the case of X representing BWC video encounters analyzed using the Mapper algorithm, a node (equivalently a cluster) represents a collection of similar encounters. This process is then repeated for $I_2, I_3, ..., I_n$.

For the dataset X shown in Figure 1, we pick three intervals to cover the range of height values, with an overlap of approximately 33%. Figure 2 shows the three intervals in the cover in green, blue, and red, as well as the preimage under the height function of each interval. Note that a particular data point in X may be in the preimage of multiple intervals, and thus may be clustered into multiple nodes. It is from such points simultaneously clustered into separate nodes that the Mapper algorithm draws its descriptive power. The algorithm draws an edge between any two nodes which share at least one such point. For a BWC video data set analyzed using the Mapper algorithm, an edge indicates that the nodes it connects represent similar types of encounters.

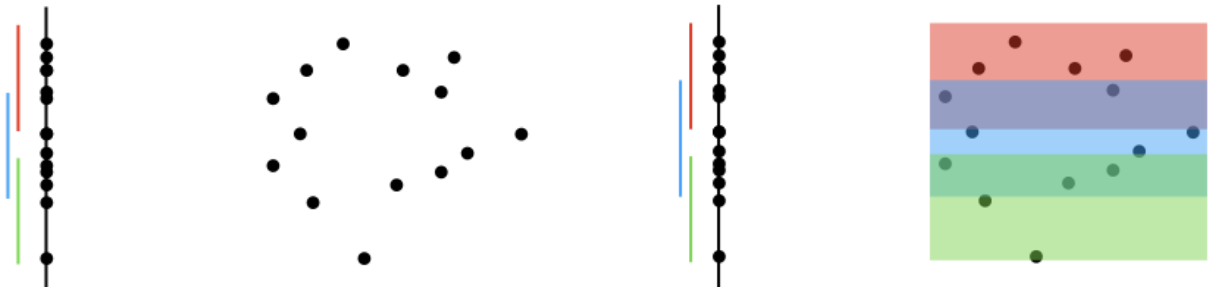

Figure 2: A cover of the (range of) height function using 3 intervals shown in green, blue, and red (left), and the preimages of the intervals in the cover (right).

To complete our illustration on the 2D data set, consider a clustering algorithm whose effect on the preimages of the three intervals is as shown in Figure 3. One such clustering algorithm could be that which combines together into a cluster all points that are within a certain distance cut-off to any other point in the subset. Note that the points in the preimage of the middle (blue) interval cluster into two separate nodes, while those in the preimages of the green and red intervals cluster into single nodes each. Based on the overlap of the four clusters (or nodes), we draw four edges to get the final object shown on the right. It is clear that the graph generated by this algorithm captures the underlying structure of the input data set X, which forms a rough circle.

Even used on the small 2D data set X, the final Mapper produced by the algorithm reduces the "size" of the data set from 14 points to 4 nodes and 4 edges. Used on more realistic datasets, the reduction in size becomes far more significant. For the sake of completeness of presentation, we reproduce in Figure 4 the result of applying the Mapper algorithm on a large sample of points from a three-dimensional model of a human hand as presented originally by Lum et al. (2013). The filter function used is the distance of each point from the base of the hand (i.e., the wrist). The clustering algorithm reduces the set of points into nodes or clusters representing connected components. The input data set consisting of several hundred points is represented by the Mapper that is a graph (a tree) with 13 nodes and 12 edges that captures the "skeleton" of the hand.

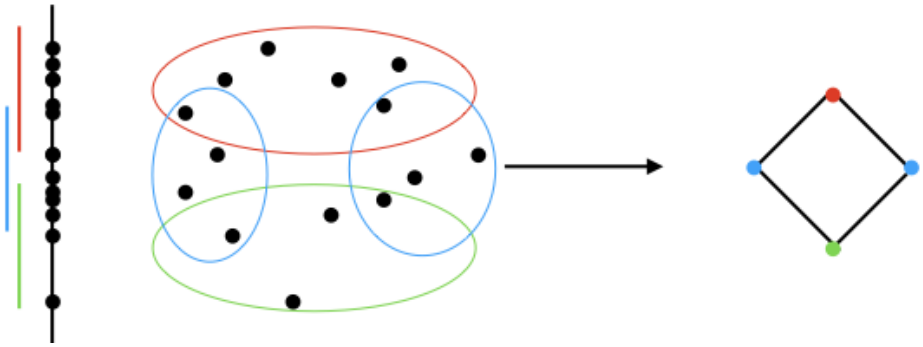

Figure 3: Clustering within intervals of the cover, and the resulting Mapper.

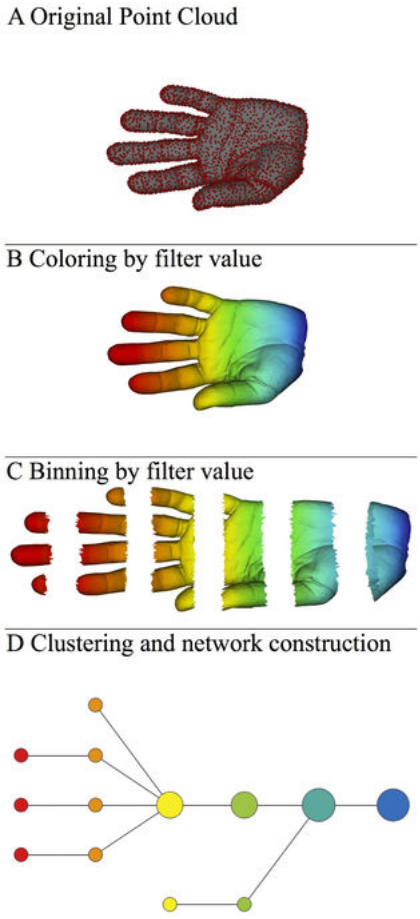

Figure 4: The Mapper representation of hundreds of points sampled from a hand. Figure taken from the work of Lum et al. (2013).

2.2.2 Options for Building the Mapper

The choices of which filter functions to try, and what values of resolution and gain (n and p) to use, are typically left to the user. Guided by the domain expert, the analyst typically tries several subsets of variables of keen interest to see which choices produce insightful Mappers (or visualizations). Multiple subsets of filter functions could naturally be tried out in parallel.

Another critical question is the "stability" of the features thus identified by a Mapper. When used over a range of values for n and p, some features will be present in graphs corresponding to many different n and p values while others will appear only in a few graphs. The wider these ranges are, the more significant the feature is. There have been some recent theoretical work that quantifies these aspects (Carrière et al., 2017; Carrière and Oudot, 2017; Dey et al., 2016). Briefly, under certain assumptions on how the data is distributed as well as how the resolution and gain are chosen, one could quantify the "stability" of the features identified by the Mapper, and also show that the overall underlying structure could be captured by the Mappers created using only a "small" subset of filter functions.

From the point of view of many applications in including that of BWC video data analysis, interesting features are places in the Mapper where paths split or join, or places where a node is adjacent to multiple nodes in some other intervals. Once we have identified such interesting features, we use statistical comparisons to determine which variable or variables differ significantly between the splitting or converging paths. These are variables which help determine which of several distinct type of encounters is likely to occur under the settings specified by the variable values of a particular data point.

Each node can now be considered as a particular subsample from the population of all clustered data points. Tools of standard statistical analysis can now compare them to each other and to the full population. In our results presented in Section 3, we use a t-test between each pair of adjacent nodes and each pair of nodes coming from the same interval when the sample sizes were large enough (with a p-value of 0.05 as the level of statistical significance).. These tests characterize how sharply two nearby nodes differ from each other. Each node is also compared to the full population to find which nodes have means differing significantly from the entire data set.

2.2.3 Preprocessing

The annotated dataset on police-citizen interactions has several categorical variables that need to be preprocessed so that we could use those variables along with the other variables with binary or continuous values. The categorical variables are typically specified as numerical values, e.g., 1–5 for a variable listing five categories. But the relative sizes of the numerical values cannot be interpreted in a quantitative manner—the members of categories 1 and 4 should not be interpreted as farther apart than members of categories 1 and 2, for instance. Hence, we decompose each categorical variable into a collection of binary variables, one per category. This way, the distance between members belonging to any two categories are measured equally. The distance metric used for filtering and clustering, like the filter function and clustering algorithm, lacks a canonical choice. Often, the Euclidean metric is a reasonable first choice, and we use the same unless mentioned otherwise.

Several variables in the data set required some further preprocessing before we could apply the Mapper algorithm. In particular, the Time-To-Force (TtF) variable recorded the length of time from the moment the police officer in the encounter identified themselves as such and the moment of first use of force. At the same time, if no force was used at all in an encounter, the TtF variable was recorded as the length of the video itself. This set up could create some confusion, as a short encounter in which no force was used could have a smaller TtF value than a longer encounter in which the first use of force occurred a longer time after the encounter started. Hence, we assigned a pre-determined TtF value for all videos in which force was not used. We chose this value large enough such that videos where force was used and videos where no force was used were not grouped together in the same interval of a cover of the TtF filter function. At the same time, this TtF value was small enough such that the Mapper framework could still identify patterns within the videos where force was used.

Once a specific Mapper representation is chosen, our basic strategy is to describe the clusters and sub-clusters identified by variables that could help explain the behavior of these subgroups. In other words, we examine the degree to which there are racial/ethnic, gender, level of aggression, etc., differences between the subpopulations.

3 Results

We present the details of the structural features in the BWC video data set extracted by the Mapper algorithm. Our focus is on the use of force in the encounters, and we employ two key variables capturing this aspect as filter functions in the Mapper algorithm—Uses of Force (UoF) and Time to Force (TtF).

3.1 Analysis of Uses of Force

The variable Uses of Force (UoF) has values in the range 0.0–14.0, with higher values indicating increased use of force in the encounter. It was a natural choice to use UoF as a filter function, as our goal is to understand the nuances of what factors determine the use of force in encounters with the police. We studied the Mappers generated over wide ranges of values of resolution and gain (n and p), while observing which ones revealed nontrivial features or structure in the data set. We observed that a Mapper representation revealing a lot of structure remained stable across the following range of values: $n \in [14, 16]$ and $p \in [0.4, 0.99]$. Hence we chose the Mapper given by $n = 15$ and $p = 0.6$ for detailed analysis, which we present in Figure 5 and describe in detail below.

We get ten nodes (i.e., clusters) in the representative Mapper (in Figure 5), which group into six subsets of clusters based on their average values of UoF (the average value is denoted $\bar{\mu}$). The clusters are labeled C_1 through C_{10}. These six groups are shown horizontally, going from an average UoF value $\bar{\mu} = 0.04$ to $\bar{\mu} = 5.0$, with the average UoF values for each group indicated at the top, therefore indicating that incidents in which force was applied more times appear further to the right in the Mapper visualization. The node sizes scale logarithmically with the number of encounters (i.e., videos) in the associated cluster. Thus, doubling the size, i.e., radius, of a node corresponds approximately to increasing the size

of the cluster by an order of magnitude. Racial distributions of suspects in the encounters belonging to each cluster is shown in a pie-chart placed within the node. We present the averages or compositions for individual variables within each cluster in Table 2.

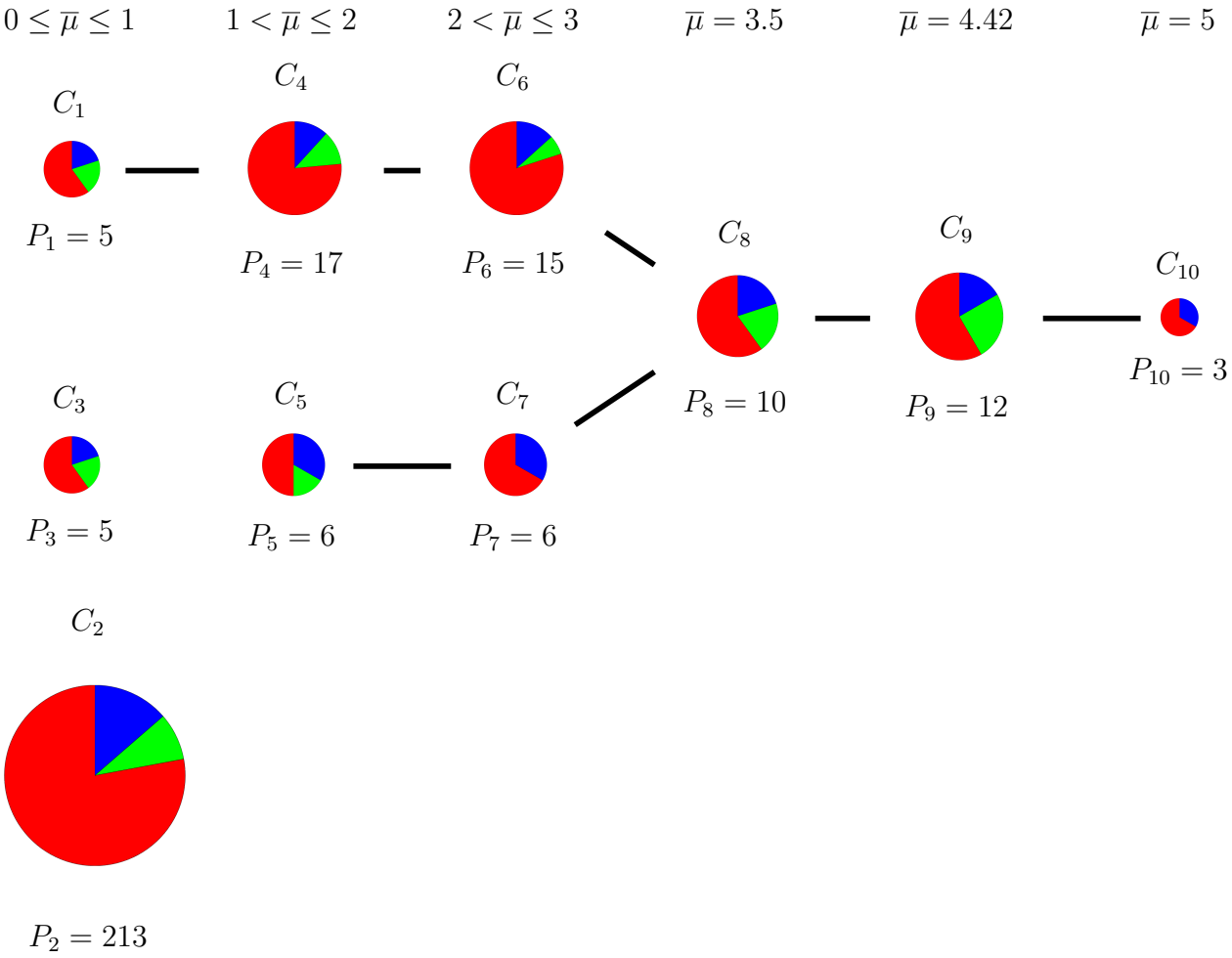

Figure 5: Representation of the BWC video data set using the variable Uses of Force (UoF) as the filter, with the racial distributions shown as pie charts inside each cluster. The percentages of suspects who are white, black, and belong to other ethnicities are shown in red, green, and blue, respectively. Vertical columns of clusters represent groups of nodes with similar average values ($\bar{\mu}$) of uses of force (ranges of values shown at top of the column). The population of cluster C_i is listed beneath the node as P_i for $i = 1, \ldots, 10$. See Section 3.1 for more details.

The most interesting feature in the UoF Mapper is the merging of the C_1-C_4-C_6-C_8 path and the C_5-C_7-C_8 path. The two parallel paths with low average UoF represent distinct types of experience. We want to know what causes some encounters to take the upper path rather than the lower path. To this end, we performed a basic statistical analysis of the compositions of nodes in each path—that is, we check the pairwise differences of C_1, C_4, C_6, and C_8 as well as the differences of C_5, C_7, and C_8. We also check the nodes in the same interval for differences—C_4 against C_5 and C_6 against C_7. The pairwise differences of average values of variables along with associated p-values for whether the differences are statistically significant are presented in Table 3. The upper path has a much higher concentration of white suspects, at 76% and 80% for nodes C_4 and C_6, respectively (C_1 has 60% white suspects, but has no corresponding node in the lower path). On the other hand, nodes C_5 and C_7 have only 50% and 66% white suspects. The entire data set of 288 videos has a mean white concentration of 76%.

Likewise, the upper path encounters have greater levels of aggression from the suspect than the ones captured in the lower path. Specifically, the upper path nodes C_4 and C_6 had 76% and 73% concentrations of medium levels of aggression from suspects, respectively, while the lower path nodes C_5 and C_7 had only 50% and 66% levels of medium aggression. High levels of aggression were largely absent in both paths.

Further, the upper path captures incidents in which police used higher levels of force than the ones in the lower path. For example, 41% and 46% of the uses of force in nodes C_4 and C_6 occurred at level 2 (grappling to maintain control of the suspect), while only 17% and 33% of uses of force reached this level for the incidents captured in nodes C_5 and C_7, which have the same average UoF value as nodes C_4 and C_6, respectively. Nodes C_4 and C_6 also had 24% and 27% of uses of force at level 4 (instrument-based force), while neither C_5 nor C_7 had any level 4 force. Similarly, the lower path has higher concentrations of low levels of force (verbal threats and pat downs) than the upper path (specifically, 66% and 50% versus 7% and 10%).

Though we also present Mapper results using Time to Force (TtF) as a filter function separately below, we explore the degree to which TtF values differ between the two paths in the UoF Mapper. The upper path has a much lower average TtF value than the lower path—force is first applied in C_4 and C_6 at about 25 seconds, while it takes 160–170 seconds for the first application of force in C_5 and C_7.

In short, the two paths appear to represent aggressive suspects with a high white concentration on the one hand, and passive suspects with a relatively low white concentration on the other hand, experiencing approximately the same number of uses of force. But the aggressive suspects tend to experience higher maximum levels of force, which is consistent with prior research indicating aggressive posturing and the demeanor of the person influence the odds force is used (Makin et al., 2018; Mastrofski et al., 2002; Klinger, 1995).

Another interesting observation is that the encounters captured in the lower path involve similar police uses of force as those in the upper path, despite low levels of resistance in the former set. While quick application of force in the encounters captured in the upper path can likely be attributed to its higher rates of aggression, it is not clear what causes force to be used along the lower path. We plan to explore this and related aspects in future studies. It should be noted that the higher aggression path experienced greater levels of force than the lower aggression path.

It is also worth noting that white suspects tended to be overrepresented in clusters C_1–C_5, which recorded low numbers of uses of force, and underrepresented in clusters C_8–C_{10} (see Table 2), which had relatively high numbers of uses of force (independent of the two paths we described earlier). A similar observation could be made about male suspects as well. While the number of encounters with high values of UoF is far smaller than those with low values of UoF, the fact that minority suspects are overrepresented while white suspects are underrepresented over the whole set of nodes suggests that this observation may not be a result of the small numbers of encounters in each node. However, the relatively small sizes of the nodes with higher UoF values makes it hard to draw statistically significant conclusions from them.

Apart from the insights presented above, other results were as one might expect: higher levels of suspect aggression correlated with more uses of force and higher maximum force levels, night interactions tended to produce more uses of force, and more uses of force generally resulted in more arrests. Male suspects also tend to be more aggressive than are females. The higher force used against male suspects could then be at least partially explained due to increased suspect aggression rather than gender. See Table 4 for the correlation coefficients.

3.2 Analysis of Time to Force

The variable Time to Force (TtF) has values in the range 0.0–1831, with higher values indicating longer wait times from the start of the encounter before the first application of force. As we mentioned in Section 2.2.3, the TtF values were preprocessed so that encounters with *no* use of force are assigned reasonable yet large TtF values when compared to TtF values from encounters that actually saw use of force. Based on the range (0.0–1291) of TtF values for encounters where force was used, we selected 1400 as the TtF value assigned to encounters that saw no use of force. This upper bound value was sufficiently distinct from the TtF values for instances where force was used so that we avoided mixing the qualitatively distinct data. At the same time, this value was still small enough to preserve distinctions among the instances in which force was used. In particular, if we were to use a much larger value, the smaller TtF values for instances where force was used would all be clumped together when computing distances based on TtF. The average TtF values for nodes where force was indeed applied remains much smaller—around 192 (see Figure 6). With this choice, the resulting Mappers truthfully captured the use of first force as measured by TtF.

Similar to Uses of Force (UoF), Time to Force (TtF) was a natural choice to use as a filter function. At the same time, the resulting Mapper representation using TtF revealed distinct patterns from that found using the UoF representation. We observed a nontrivial Mapper representation was stable across the following ranges of values of resolution and gain: $n \in [33, 43]$ and $p \in [0.5, 0.99]$. Hence we chose the Mapper given by $n = 40$ and $p = 0.6$ for detailed analysis, which we present in Figure 6 and describe the details below.

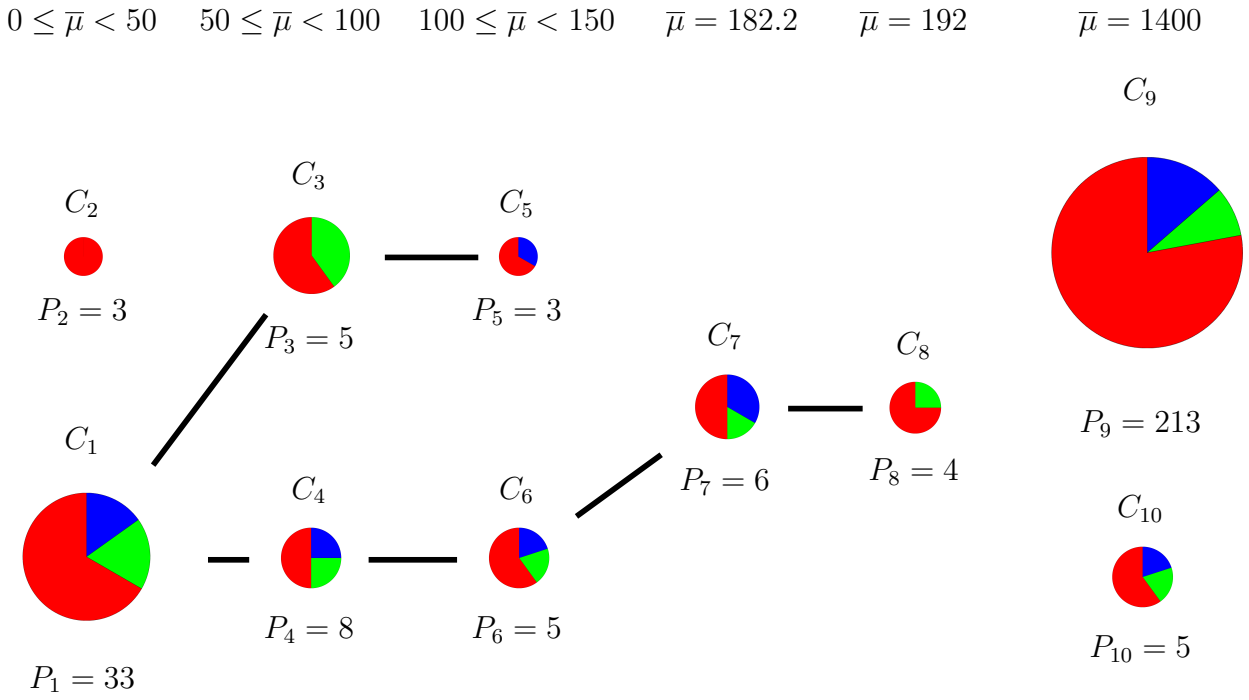

Figure 6: Representation of the BWC video data set using the variable Time to Force (TtF), with the racial distributions shown as pie charts inside each cluster. Percentage of suspects who are white, black, and from other ethnicities are shown in red, green, and blue, respectively. Vertical columns of nodes represent clusters with similar average TtF values (indicated by $\bar{\mu}$). The average TtF values for each column is noted above. The population size of cluster C_i is listed beneath that node as P_i for $i = 1, \ldots, 10$.

The Mapper representation produced by the Time to Force filter function contained ten clusters in six distinct subsets based on average TtF (see Figure 6). The clusters are labeled C_1–C_{10}. We present the averages or compositions for individual variables within each cluster in Table 5. We also present pairwise differences of average values of variables and associated p-values for whether the differences are significant for relevant pairs of nodes in Table 6.

While many of the nodes in the TtF visualization have small sizes that drawing statistically significant conclusions might be difficult, it is important to note that minority suspects (belonging to African-American or other ethnicities) are significantly represented in every node in which force is used except for the three suspects in C_2.

The small sizes of many of the nodes notwithstanding, we make the following interesting observations from the TtF Mapper. First, the compositions of C_9 and C_{10}, the two nodes capturing encounters that saw no use of force, differ in meaningful ways. Node C_9, containing a large majority (213 out of 288) of encounters in the data set, is quite close to the population mean for the racial distribution of suspects, having 78% white suspects, 8% black suspects and 14% suspects of other races while the population has 76% white suspects, 10% black suspects, and 14% suspects of other races. While close to the population average, minority suspects are slightly underrepresented and white suspects slightly overrepresented (compared to the overall population). In C_{10}, minority suspects are slightly overrepresented, as 20% of its members are black and 20% are of other minority races, as compared to the population averages given above.

More interestingly, only 40% of the members of C_{10} were male—which is far less than the corresponding concentration of C_9 (68%), let alone that of the overall population (71%). Indeed, this is the only node where females outnumber males. We also point out that no members of C_{10} were arrested, a fact true of only 76% of members of C_9 and 71% of the entire population. Likewise, members of C_{10} were uniformly non-aggressive while C_9 contains members who displayed medium (13%) or even high (1%) aggression.

In summary, there appear to be two classes of suspects who do not have any force used against them. The first larger class is the average class, generally near the population mean, though generally lower on aggression and with a higher concentration of females. The second class is a predominantly female group with a higher concentration of minority suspects who behave perfectly (in that they are non-aggressive and are not arrested). This observation suggests that minority suspects may have to be members of a perceived nonthreatening group (women) and be on good behavior (non-aggressive and not appearing to commit a crime) to avoid aggression. At the same time, higher concentrations of white suspects can get away with actions that are more aggressive, suspicious behaviors, or being male, without having force used against them. As the small sample size of C_{10} limits how certain we can be in this conclusion, additional work with large samples is warranted.

The divisions of clusters in the first three sets (that is, the divisions between C_1 and C_2, C_3 and C_4, as well as C_5 and C_6) reflect a significant difference in the duration of force. Clusters C_2, C_3, and C_5 have much higher durations of force than their counterparts in the lower path. Node C_5 has an average of almost 2.5 times the duration of force of C_6, while Node C_3 has nearly 4 times the duration of force as that of C_4, and over 6 times that experienced in C_1. The causes of these differences are unclear, and merits further investigation. A larger data set might make some causal trend visible, or there may be some other variable not reported as part of the current data set causing this difference.

4 Discussion

The application of the Mapper algorithm to the annotated BWC footage of 288 incidents demonstrates the utility of topological data analysis to the study of police interactions specifically and to the study of criminal justice more broadly. Examining both Uses of Force (UoF) and Time to Force (TtF), our analysis produced Mapper representations showing that there are specific clusters and subsets of clusters that describe distinct types of incidents in which force is used and how quickly force tends to be applied in police-community interactions. Though there are a number of methods available for analyzing and identifying clusters from a whole data set, the results presented here are distinct as they identify families of clusters that show nontrivial trends that could not be identified using traditional methods.

For UoF, our analysis revealed 10 different clusters or types of encounters that can be divided up over 6 different levels of force. These results reveal that incidents involving multiple uses of force are relatively rare in police-community encounters, but when they do occur, they tend to include a disproportionately large fraction of minorities, men, and aggressive suspects. Similarly, the results on TtF also resulted in 6 distinct subsets and 10 different nodes. These clusters reveal that force is typically used more quickly against Black suspects (evidenced by the increased fractions of Black suspects in the videos captured by nodes C_1, C_3, and C_4 when compared to the overall population). But perhaps more importantly, these results identified interesting patterns in who does *not* have force used against them. Though all of these results must be tempered by the sample size and the generalizability of the data, taken together, the Mapper visualizations support much of the prior literature on use of force while revealing a more nuanced picture of how uses of force is experienced. In particular, race, gender, and aggression on the part of the suspects seem to shape police-community interactions and can be used to help explain how police encounters form into distinct sets and subsets of encounter types. Importantly, while these data do suggest a difference in how force is used, these results do not take into consideration broader contextual factors. Police-community interactions are inherently complex and the purpose of the present study is to understand the contours shaping these interactions through a narrowed analysis of use of force. As Makin et al. (2018) show in their recent study modeling use of force and race, when additional situational, environmental, and organizational factors are introduced into the models, the race of the community member lessens in significance and power becoming nonsignificant in explaining if, and how use of force occurs.

4.1 Limitations and Future Research

As a proof-of-concept, we caution against generalizing our results, though our results do mirror many of the prior findings on use of force and gender. Our TDA approach is, by design, not a predictive tool. If the goal is to build predictive models to assist with identifying the plausible behavior of encounters in the future, we could use standard regression or machine learning techniques on top of the analysis we have undertaken here. We present TDA in hopes of introducing a new computational approach to inform how we model complex data sets, which as we have demonstrated will inevitably come to rely upon annotated BWC footage. TDA holds tremendous value in assisting researchers to separate complex data sets with dynamic variables into meaningful clusters that could not be achieved using traditional

approaches. Human interactions are a composite of a myriad of different events that often are dynamically interrelated, and the frequency and intensity of those interactions may shape the ultimate outcome. In this setting, TDA provides a strategy for visualizing complex dynamic events into more easily interpreted representations for researchers. In particular, we believe that a TDA analysis of a larger data set with additional contextual information such as location of contact, time of contact, environment, presence of bystanders, behavioral cues of the suspect (i.e., resistance and type of resistance), and the subsequent time points and duration of each associated event would constitute an important first step toward comprehensively deconstructing police-citizen interactions. Using this TDA approach, researchers could identify the specific classification of interactions where techniques such as de-escalation are successful and those where specific techniques may escalate a situation. Such an analysis would progress the development and evaluation of training and interventions to a point where practitioners and policy makers would have empirical data associated with efficacious practices. Similarly, having access to other variables of interest, e.g., heart rate readings of the officer, could allow us to identify and explain further details and nuances of how interactions with police evolve.

5 Conclusion

Social interactions are complex phenomena that, when studied at the situational-level, can produce a wealth of data which is difficult to examine. Police-community interactions are similarly difficult to analyze and, given the high-stakes associated with such encounters, perhaps even more important to study. Several scholars have recently argued that criminology has failed to tackle the challenge of exploring situational interactions (Collins, 2009; Wikström et al., 2012). We agree with this general sentiment, and argue that examining police-interactions at the situational-level requires specialized data and advanced data analysis techniques. Our goal in this paper was to provide a demonstration of how annotated BWC data could be used to study issues related to police use of force, and to provide an illustration of the type of insights that can be gained from the use of topological data analysis. It is not our intent to produce generalizable results. The data we used originates from a small subset of police interactions from a single agency, and we used the same to demonstrate the viability of using the Mapper algorithm to identify a series of discrete subpopulations within the set of use of force events.

Table 2: Averages/Concentrations of the 10 nodes in the Uses of Force (UoF) Mapper presented in Figure 5. The last column (Pop) gives the average values for the entire data set (population). (Low,Med,Hi)_Aggr represents low, medium, and high aggression. Lev$i$_Force represents the fractions of level-i force for $i = 1, 2, 3, 4$. Avg_LoF_Mn and Avg_LoF_Sum represent the average (within the cluster) of the duration (length) of force means and the duration of force sums. Avg_Force$i$ represents the average durations of Level i force for $i = 1, 2, 3, 4$. Avg_Duration represents the average of overall duration of force. Data_Points gives the sizes of the clusters (i.e., number of videos in each node).

↓Var/Node→	C_1	C_2	C_3	C_4	C_5	C_6	C_7	C_8	C_9	C_{10}	Pop
White	0.60	0.78	0.60	0.76	0.50	0.80	0.67	0.60	0.58	0.67	0.76
Black	0.20	0.08	0.20	0.12	0.17	0.07	0.00	0.20	0.25	0.00	0.10
Other	0.20	0.14	0.20	0.12	0.33	0.13	0.33	0.20	0.17	0.33	0.14
Low_Aggr	0.00	0.86	1.00	0.18	0.50	0.27	0.33	0.20	0.17	0.00	0.77
Med_Aggr	1.00	0.13	0.00	0.76	0.50	0.73	0.67	0.70	0.58	0.67	0.21
Hi_Aggr	0.00	0.01	0.00	0.06	0.00	0.00	0.00	0.10	0.25	0.33	0.02
No_Force	0.00	1.00	1.00	0.00	0.00	0.00	0.00	0.00	0.00	0.00	0.84
Lev1_Force	0.60	0.00	0.00	0.18	0.67	0.07	0.50	0.10	0.08	0.00	0.03
Lev2_Force	0.20	0.00	0.00	0.41	0.17	0.47	0.33	0.60	0.33	0.33	0.06
Lev3_Force	0.00	0.00	0.00	0.18	0.17	0.20	0.17	0.00	0.25	0.67	0.03
Lev4_Force	0.20	0.00	0.00	0.24	0.00	0.27	0.00	0.30	0.33	0.00	0.03
Male	0.80	0.68	0.40	0.88	0.83	0.93	0.67	0.90	1.00	1.00	0.71
Female	0.20	0.32	0.60	0.12	0.17	0.07	0.33	0.10	0.00	0.00	0.29
Day	0.00	0.38	0.00	0.18	0.00	0.27	0.00	0.10	0.00	0.00	0.33
Night	1.00	0.62	1.00	0.82	1.00	0.73	1.00	0.90	1.00	1.00	0.67
Arrest	0.40	0.23	1.00	0.59	0.17	0.47	0.17	0.40	0.75	1.00	0.27
No_arrest	0.60	0.77	0.00	0.41	0.83	0.53	0.83	0.60	0.25	0.00	0.71
Avg_UoF	1.00	0.00	0.00	1.65	1.83	2.27	2.17	3.50	4.42	5.00	0.41
Avg_LoF_Mn	1.80	0.00	0.00	2.03	1.42	1.97	1.47	1.61	1.68	1.47	0.27
Avg_LoF_Sum	1.80	0.00	0.00	3.41	2.67	4.33	3.17	5.70	7.42	7.33	0.72
Avg_Force1	0.60	0.00	0.00	0.65	1.17	1.07	1.33	2.10	2.67	3.33	0.23
Avg_Force2	0.20	0.00	0.00	0.53	0.50	0.67	0.67	0.90	0.92	1.00	0.10
Avg_Force3	0.00	0.00	0.00	0.18	0.17	0.20	0.17	0.20	0.42	0.67	0.03
Avg_Force4	0.20	0.00	0.00	0.29	0.00	0.33	0.00	0.30	0.42	0.00	0.04
Avg_Duration	19.0	0.00	0.00	47.2	50.8	58.1	54.2	56.2	95.5	98.0	10.0
Avg_TtF	35.2	1400	1400	26.1	168.8	22.8	160.3	40.6	46.7	14.7	1192
Data_Points	5	213	5	17	6	15	6	10	12	3	258

Table 3: Pairwise differences of averages/concentrations between nodes in the UoF Mapper (presented in Figure 5), and the associated p-Values for whether the differences are statistically significant in braces. The variables appear in the columns in the same order as listed in Table 2 (except for Data_Points). For the pair $\{C_i, C_j\}$, the difference listed is the value of the variable for C_i minus the value for C_j. The p-value is undefined (listed as $(\times)$) when there are no instances of that variable observed in at least one of the two nodes in question.

	White	Black	Other	Low_Aggr	Med_Aggr	Hi_Aggr	No_Frc	L1_Frc	L2_Frc	L3_Frc	L4_Frc	Male	Fml
C_1, C_4	−0.16 (0.6)	0.08 (0.7)	0.08 (0.7)	−0.18 (0.1)	0.24 (0.04)	−0.06 (0.3)	0 (×)	0.42 (0.2)	−0.21 (0.4)	−0.18 (0.1)	−0.04 (0.9)	−0.08 (0.7)	0.08 (0.7)
C_4, C_6	−0.04 (0.8)	0.05 (0.6)	−0.02 (0.9)	−0.09 (0.6)	0.03 (0.8)	0.06 (0.3)	0 (×)	0.11 (0.4)	−0.05 (0.8)	−0.02 (0.9)	−0.03 (0.8)	−0.05 (0.6)	0.05 (0.6)
C_5, C_7	−0.17 (0.6)	0.17 (0.4)	0 (1.0)	0.17 (0.6)	−0.17 (0.6)	0 (×)	0 (×)	0.17 (0.6)	−0.17 (0.6)	0 (1.0)	0 (×)	0.17 (0.6)	−0.17 (0.6)
C_6, C_8	0.2 (0.3)	−0.13 (0.4)	−0.07 (0.7)	0.07 (0.7)	0.03 (0.9)	−0.1 (0.3)	0 (×)	−0.03 (0.8)	−0.13 (0.5)	0.2 (0.1)	−0.03 (0.9)	0.03 (0.8)	−0.03 (0.8)
C_7, C_8	0.07 (0.8)	−0.2 (0.2)	0.13 (0.6)	0.13 (0.6)	−0.03 (0.9)	−0.1 (0.3)	0 (×)	0.4 (0.2)	−0.27 (0.3)	0.17 (0.4)	−0.3 (0.1)	−0.23 (0.4)	0.23 (0.4)
C_8, C_9	0.02 (0.9)	−0.05 (0.8)	0.03 (0.9)	0.03 (0.9)	0.12 (0.6)	−0.15 (0.4)	0 (×)	0.02 (0.9)	0.27 (0.2)	−0.25 (0.1)	−0.03 (0.9)	−0.1 (0.3)	0.1 (0.3)
C_9, C_{10}	−0.08 (0.8)	0.25 (0.1)	−0.17 (0.7)	0.17 (0.2)	−0.08 (0.8)	−0.08 (0.8)	0 (×)	0.08 (0.3)	0 (1.0)	−0.42 (0.3)	0.33 (0.04)	0 (×)	0 (×)
C_1, C_2	−0.18 (0.5)	0.12 (0.6)	0.06 (0.8)	−0.86 (0)	0.87 (0)	−0.01 (0.2)	−1 (0)	0.6 (0.1)	0.2 (0.4)	0 (×)	0.2 (0.4)	0.12 (0.6)	−0.12 (0.6)
C_1, C_3	0 (1.0)	0 (1.0)	0 (1.0)	−1 (0)	1 (0)	0 (×)	−1 (0)	0.6 (0.1)	0.2 (0.4)	0 (×)	0.2 (0.4)	0.4 (0.2)	−0.4 (0.2)
C_2, C_3	0.18 (0.5)	−0.12 (0.6)	−0.06 (0.8)	−0.14 (0)	0.13 (0)	0.01 (0.2)	0 (×)	0 (×)	0 (×)	0 (×)	0 (×)	0.28 (0.3)	−0.28 (0.3)
C_4, C_5	0.26 (0.3)	−0.05 (0.8)	−0.22 (0.4)	−0.32 (0.2)	0.26 (0.3)	0.06 (0.3)	0 (×)	−0.49 (0.1)	0.25 (0.3)	0.01 (1.0)	0.24 (0.04)	0.05 (0.8)	−0.05 (0.8)
C_6, C_7	0.13 (0.6)	0.07 (0.3)	−0.2 (0.4)	−0.07 (0.8)	0.07 (0.8)	0 (×)	0 (×)	−0.43 (0.1)	0.13 (0.6)	0.03 (0.9)	0.27 (0.04)	0.27 (0.3)	−0.27 (0.3)

	Day	Night	Arst	No_Arst	Av_UoF	Av_LoFMn	Av_LoFSm	Av_F1	Av_F2	Av_F3	Av_F4	Av_Drn	Av_TtF
C_1, C_4	−0.18 (0.1)	0.18 (0.1)	−0.19 (0.5)	0.19 (0.5)	−0.65 (0)	−0.23 (0.7)	−1.61 (0.05)	−0.05 (0.9)	−0.33 (0.2)	−0.18 (0.1)	−0.09 (0.7)	−28.18 (0.03)	9.08 (0.6)
C_4, C_6	−0.09 (0.6)	0.09 (0.6)	0.12 (0.5)	−0.12 (0.5)	−0.62 (0)	0.06 (0.8)	−0.92 (0.1)	−0.42 (0.1)	−0.14 (0.6)	−0.02 (0.9)	−0.04 (0.9)	−10.96 (0.5)	3.32 (0.7)
C_5, C_7	0 (×)	0 (×)	0 (1.0)	0 (1.0)	−0.33 (0.2)	−0.06 (0.9)	−0.5 (0.6)	−0.17 (0.8)	−0.17 (0.7)	0 (1.0)	0 (×)	−3.33 (0.9)	8.5 (0.7)
C_6, C_8	0.17 (0.3)	−0.17 (0.3)	0.07 (0.8)	−0.07 (0.8)	−1.23 (0)	0.36 (0.1)	−1.37 (0.1)	−1.03 (0)	−0.23 (0.5)	0 (1.0)	0.03 (0.9)	1.93 (0.9)	−17.8 (0.3)
C_7, C_8	−0.1 (0.3)	0.1 (0.3)	−0.23 (0.3)	0.23 (0.3)	−1.33 (0)	−0.14 (0.7)	−2.53 (0.01)	−0.77 (0.2)	−0.23 (0.6)	−0.03 (0.9)	−0.3 (0.1)	−2.03 (0.9)	119.73 (0)
C_8, C_9	0.1 (0.3)	−0.1 (0.3)	−0.35 (0.1)	0.35 (0.1)	−0.92 (0)	−0.07 (0.8)	−1.72 (0.1)	−0.57 (0.1)	−0.02 (1.0)	−0.22 (0.3)	−0.12 (0.6)	−39.3 (0.04)	−6.07 (0.7)
C_9, C_{10}	0 (×)	0 (×)	−0.25 (0.1)	0.25 (0.1)	−0.58 (0)	0.21 (0.3)	0.08 (0.9)	−0.67 (0.2)	−0.08 (0.6)	−0.25 (0.5)	0.42 (0.05)	−2.5 (0.9)	32 (0.04)
C_1, C_2	−0.38 (0)	0.38 (0)	0.17 (0.5)	−0.17 (0.5)	1 (0)	1.8 (0.04)	1.8 (0.04)	0.6 (0.1)	0.2 (0.4)	0 (×)	0.2 (0.4)	19 (0.03)	−1364.8 (0)
C_1, C_3	0 (×)	0 (×)	0.4 (0.2)	0.6 (0.1)	1 (0)	1.8 (0.04)	1.8 (0.04)	0.6 (0.1)	0.2 (0.4)	0 (×)	0.2 (0.4)	19 (0.03)	−1364.8 (0)
C_2, C_3	0.38 (0)	−0.38 (0)	0.23 (0)	0.77 (0)	0 (×)	0 (×)	0 (×)	0 (×)	0 (×)	0 (×)	0 (×)	0 (×)	0 (×)
C_4, C_5	0.18 (0.1)	−0.18 (0.1)	0.42 (0.1)	−0.42 (0.1)	−0.19 (0.4)	0.61 (0.1)	0.75 (0.3)	−0.52 (0.3)	0.03 (0.9)	0.01 (1.0)	0.29 (0.1)	−3.66 (0.8)	−142.72 (0)
C_6, C_7	0.27 (0.04)	−0.27 (0.04)	0.3 (0.2)	−0.3 (0.2)	0.1 (0.6)	0.49 (0.2)	1.17 (0.1)	−0.27 (0.6)	0 (1.0)	0.03 (0.9)	0.33 (0.1)	3.97 (0.8)	−137.53 (0)

Table 4: Correlation coefficients between variables measuring Aggression, Levels of Force, Night, Male, and Average UoF for the entire BWC data set. The variables names are explained in Table 2.

	No_Force	Lev1_Force	Lev2_Force	Lev3_Force	Lev4_Force	Male	Avg_UoF
Low_Aggr	0.90	−0.23	−0.72	−0.49	−0.54	−0.81	
Med_Aggr	−0.90	0.43	0.70	0.24	0.54	0.68	
Hi_Aggr	−0.31	−0.43	0.31	0.79	0.17	0.62	
Male	−0.77	−0.04	0.69	0.57	0.58	1.00	
Night	−0.38	0.44	0.03	0.26	−0.10		0.37
Arrest							0.32

Table 5: Averages/Concentrations of the 10 nodes in the Time to Force (TtF) Mapper presented in Figure 6. The last column (Pop) gives the average values for the entire data set (population). Variables are same as ones listed in Table 2, the corresponding table for UoF.

↓Var/Node→	C_1	C_2	C_3	C_4	C_5	C_6	C_7	C_8	C_9	C_{10}	Pop
White	0.67	1.00	0.60	0.50	0.67	0.60	0.50	0.75	0.78	0.60	0.76
Black	0.18	0.00	0.40	0.25	0.00	0.20	0.17	0.25	0.08	0.20	0.10
Other	0.15	0.00	0.00	0.25	0.33	0.20	0.33	0.00	0.14	0.20	0.14
Low_Aggr	0.18	0.33	0.20	0.13	0.33	0.20	0.50	0.50	0.86	1.00	0.75
Med_Aggr	0.73	0.67	0.80	0.63	0.00	0.60	0.50	0.50	0.13	0.00	0.22
Hi_Aggr	0.09	0.00	0.00	0.25	0.67	0.20	0.00	0.00	0.01	0.00	0.03
No_force	0.00	0.00	0.00	0.00	0.00	0.00	0.00	0.00	1.00	1.00	0.82
Lev1_force	0.12	0.33	0.20	0.13	0.33	0.20	0.50	0.75	0.00	0.00	0.04
Lev2_force	0.45	0.33	0.20	0.50	0.00	0.20	0.17	0.00	0.00	0.00	0.07
Lev3_force	0.18	0.00	0.40	0.00	0.33	0.20	0.33	0.25	0.00	0.00	0.03
Lev4_force	0.24	0.33	0.20	0.38	0.33	0.40	0.00	0.00	0.00	0.00	0.04
Male	0.94	0.67	1.00	1.00	1.00	0.80	0.83	0.75	0.68	0.40	0.72
Female	0.06	0.33	0.00	0.00	0.00	0.20	0.17	0.25	0.32	0.60	0.28
Day	0.12	0.33	0.00	0.13	0.00	0.00	0.00	0.00	0.38	0.00	0.33
Night	0.88	0.67	1.00	0.88	1.00	1.00	1.00	1.00	0.62	1.00	0.67
Arrest	0.61	0.67	0.80	0.75	1.00	0.40	0.17	0.25	0.23	1.00	0.29
No_Arrest	0.39	0.33	0.20	0.25	0.00	0.60	0.83	0.75	0.77	0.00	0.69
Avg_UoF	2.85	3.67	3.40	2.63	8.67	3.20	2.33	2.50	0.00	0.00	0.60
Avg_LoF_Mn	1.79	1.27	1.61	2.05	1.38	1.90	1.48	1.10	0.00	0.00	0.31
Avg_LoF_Sum	4.82	5.00	5.40	5.13	13.0	6.40	3.50	3.00	0.00	0.00	0.98
Avg_Force1	1.64	3.00	2.20	1.25	6.67	1.60	1.50	2.25	0.00	0.00	0.37
Avg_Force2	0.73	0.33	0.60	0.75	0.33	0.60	0.50	0.00	0.00	0.00	0.12
Avg_Force3	0.21	0.00	0.40	0.13	1.00	0.40	0.33	0.25	0.00	0.00	0.05
Avg_Force4	0.27	0.33	0.20	0.50	0.67	0.60	0.00	0.00	0.00	0.00	0.06
Avg_Duration	75.7	462.3	177.2	45.6	174	72.6	52.5	55.0	0.00	0.00	18.7
Avg_TtF	25.7	20.3	64.2	78.4	134	122	182	192	1400	1400	1154
Data_Points	33	3	5	8	3	5	6	4	213	5	267

Table 6: Pairwise differences of averages/concentrations between nodes in the TtF Mapper (presented in Figure 6), and the associated p-Values for whether the differences are statistically significant in braces. The variables appear in the columns in the same order as listed in Table 5 (except fo Data_Points). For the pair $\{C_i, C_j\}$, the difference listed is the value of the variable for C_i minus the value for C_j. The p-value is undefined (listed as $(\times)$) when there are no instances of that variable observed in at least one of the two nodes in question.

	White	Black	Other	Low_Aggr	Med_Aggr	Hi_Aggr	No_Frc	L1_Frc	L2_Frc	L3_Frc	L4_Frc	Male	Fml
C_1, C_3	0.07 (0.8)	−0.22 (0.4)	0.15 (0.02)	−0.02 (0.9)	−0.07 (0.8)	0.09 (0.1)	0 (×)	−0.08 (0.7)	0.25 (0.3)	−0.22 (0.4)	0.04 (0.9)	−0.06 (0.2)	0.06 (0.2)
C_1, C_4	0.17 (0.4)	−0.07 (0.7)	−0.1 (0.6)	0.06 (0.7)	0.1 (0.6)	−0.16 (0.4)	0 (×)	0 (1.0)	−0.05 (0.8)	0.18 (0.01)	−0.13 (0.5)	−0.06 (0.2)	0.06 (0.2)
C_3, C_5	−0.07 (0.9)	0.4 (0.2)	−0.33 (0.4)	−0.13 (0.8)	0.8 (0.02)	−0.67 (0.2)	0 (×)	−0.13 (0.8)	0.2 (0.4)	0.07 (0.9)	−0.13 (0.8)	0 (×)	0 (×)
C_4, C_6	−0.1 (0.8)	0.05 (0.9)	0.05 (0.9)	−0.08 (0.8)	0.03 (0.9)	0.05 (0.9)	0 (×)	−0.08 (0.8)	0.3 (0.3)	−0.2 (0.4)	−0.03 (0.9)	0.2 (0.4)	−0.2 (0.4)
C_6, C_7	0.1 (0.8)	0.03 (0.9)	−0.13 (0.7)	−0.3 (0.3)	0.1 (0.8)	0.2 (0.4)	0 (×)	−0.3 (0.3)	0.03 (0.9)	−0.13 (0.7)	0.4 (0.2)	−0.03 (0.9)	0.03 (0.9)
C_7, C_8	−0.25 (0.5)	−0.08 (0.8)	0.33 (0.2)	0 (1)	0 (1)	0 (×)	0 (×)	−0.25 (0.5)	0.17 (0.36)	0.08 (0.8)	0 (×)	0.08 (0.8)	−0.08 (0.8)
C_1, C_2	−0.33 (0)	0.18 (0.01)	0.15 (0.02)	−0.15 (0.7)	0.06 (0.9)	0.09 (0.1)	0 (×)	−0.21 (0.6)	0.12 (0.8)	0.18 (0.01)	−0.09 (0.8)	0.27 (0.5)	−0.27 (0.5)
C_3, C_4	0.1 (0.8)	0.15 (0.6)	−0.25 (0.2)	0.08 (0.8)	0.18 (0.5)	−0.25 (0.2)	0 (×)	0.08 (0.8)	−0.3 (0.3)	0.4 (0.2)	−0.18 (0.5)	0 (×)	0 (×)
C_5, C_6	0.07 (0.9)	−0.2 (0.4)	0.13 (0.8)	0.13 (0.8)	−0.6 (0.1)	0.47 (0.3)	0 (×)	0.13 (0.8)	−0.2 (0.4)	0.13 (0.8)	−0.07 (0.9)	0.2 (0.4)	−0.2 (0.4)
C_9, C_{10}	0.18 (0.5)	−0.12 (0.6)	−0.06 (0.8)	−0.14 (0)	0.13 (0)	0.01 (0.2)	0 (×)	0 (×)	0 (×)	0 (×)	0 (×)	0.28 (0.3)	−0.28 (0.3)

	Day	Night	Arst	No_Arst	Av_UoF	Av_LoFMn	Av_LoFSm	Av_F1	Av_F2	Av_F3	Av_F4	Av_Drn	Av_TtF
C_1, C_3	0.12 (0.04)	−0.12 (0.04)	−0.19 (0.4)	0.19 (0.4)	−0.55 (0.4)	0.18 (0.4)	−0.58 (0.7)	−0.56 (0.4)	0.13 (0.7)	−0.19 (0.5)	0.07 (0.8)	−101.47 (0)	−38.5 (0.01)
C_1, C_4	0 (1.0)	0 (1.0)	−0.14 (0.5)	0.14 (0.5)	0.22 (0.7)	−0.26 (0.5)	−0.31 (0.8)	0.39 (0.4)	−0.02 (0.9)	0.09 (0.6)	−0.23 (0.4)	30.1 (0.1)	−52.7 (0)
C_3, C_5	0 (×)	0 (×)	−0.2 (0.4)	0.2 (0.4)	−5.27 (0.2)	0.23 (0.4)	−7.6 (0.3)	−4.47 (0.1)	0.27 (0.6)	−0.6 (0.4)	−0.47 (0.6)	3.2 (0.8)	−69.8 (0.03)
C_4, C_6	0.13 (0.4)	−0.13 (0.4)	0.35 (0.3)	−0.35 (0.3)	−0.58 (0.5)	0.15 (0.7)	−1.28 (0.6)	−0.35 (0.6)	0.15 (0.7)	−0.28 (0.4)	−0.1 (0.8)	−26.98 (0.1)	−43.83 (0.01)
C_6, C_7	0 (×)	0 (×)	0.23 (0.5)	−0.23 (0.5)	0.87 (0.3)	0.41 (0.3)	2.9 (0.2)	0.1 (0.9)	0.1 (0.8)	0.07 (0.8)	0.6 (0.2)	20.1 (0.3)	−60.0 (0)
C_7, C_8	0 (×)	0 (×)	−0.08 (0.8)	0.08 (0.8)	−0.17 (0.9)	0.38 (0.2)	0.5 (0.8)	−0.75 (0.4)	0.5 (0.2)	0.08 (0.8)	0 (×)	−2.5 (0.9)	−9.83 (0.2)
C_1, C_2	−0.21 (0.6)	0.21 (0.6)	−0.06 (0.9)	0.06 (0.9)	−0.82 (0.6)	0.52 (0.1)	−0.18 (0.9)	−1.36 (0.3)	0.39 (0.4)	0.21 (0.01)	−0.06 (0.9)	−386.6 (0)	5.33 (0.8)
C_3, C_4	−0.13 (0.4)	0.13 (0.4)	0.05 (0.9)	−0.05 (0.9)	0.78 (0.4)	−0.44 (0.3)	0.28 (0.9)	0.95 (0.2)	−0.15 (0.7)	0.28 (0.4)	−0.3 (0.4)	131.58 (0)	−14.18 (0.3)
C_5, C_6	0 (×)	0 (×)	0.6 (0.1)	−0.6 (0.1)	5.47 (0.2)	−0.52 (0.2)	6.6 (0.4)	5.07 (0.1)	−0.27 (0.6)	0.6 (0.4)	0.07 (0.9)	101.4 (0)	11.8 (0.6)
C_9, C_{10}	0.38 (0)	−0.38 (0)	0.23 (0)	0.77 (0)	0 (×)	0 (×)	0 (×)	0 (×)	0 (×)	0 (×)	0 (×)	0 (×)	0 (×)

Acknowledgment

Krishnamoorthy acknowledges funding from the National Science Foundation (NSF) via grant DBI-1661348.

References

Alagappan, M. (2012). From 5 to 13: Redefining the positions in basketball. In *MIT Sloan Sports Analytics Conference*. http://www.sloansportsconference.com/content/the-13-nba-positions-using-topology-to-identify-the-different-types-of-players/.

Anscombe, F. J. (1973). Graphs in statistical analysis. In *Am. Stat.*, pages 17–21.

Berk, R. (2004). *Regression Analysis: A Constructive Critique*. SAGE Publications, Inc.

Berk, R. (2010). What you can and can't properly do with regression. *Journal of Quantitative Criminology*, 26(4):481–487.

Carlsson, G. (2009). Topology and data. *Bulletin of the American Mathematical Society*, 46(2):255–308.

Carrière, M., Michel, B., and Oudot, S. (2017). Statistical analysis and parameter selection for mapper. arXiv:1706.00204.

Carrière, M. and Oudot, S. (2017). Structure and stability of the one-dimensional mapper. *Foundations of Computational Mathematics*. arXiv:1511.05823.

Cesario, J., Johnson, D. J., and Terrill, W. (2018). Is there evidence of racial disparity in police use of deadly force? Analyses of officer-involved fatal shootings in 2015–2016. *Social Psychological and Personality Science*.

Collins, R. (2009). *Violence: A Micro-sociological Theory*. Greenwood Publishing Group.

Dey, T. K., Mémoli, F., and Wang, Y. (2016). Multiscale mapper: Topological summarization via codomain covers. In *Proceedings of the Twenty-Seventh Annual ACM-SIAM Symposium on Discrete Algorithms*, SODA '16, pages 997–1013, Philadelphia, PA, USA. Society for Industrial and Applied Mathematics. arXiv:1504.03763.

Fryer, Jr, R. G. (2016). An empirical analysis of racial differences in police use of force. Working Paper 22399, National Bureau of Economic Research.

Gau, J. M., Mosher, C., and Pratt, T. C. (2010). An inquiry into the impact of suspect race on police use of tasers. *Police Quarterly*, 13(1):27–48.

Hinks, T. S., Zhou, X., Staples, K. J., Dimitrov, B. D., Manta, A., Petrossian, T., Lum, P. Y., Smith, C. G., Ward, J. A., Howarth, P. H., Walls, A. F., Gadola, S. D., and DjukanoviÄĞ, R. (2015). Innate and adaptive T cells in asthmatic patients: Relationship to severity and disease mechanisms. *Journal of Allergy and Clinical Immunology*, 136(2):323–333.

Holmes, M. D. and Smith, B. W. (2008). *Race and Police Brutality: Roots of an Urban Dilemma*. SUNY Press.

Jackson, B. A. (2015). Respect and legitimacy—A two-way street: Strengthening trust between police and the public in an era of increasing transparency. Rand Corporation. 28 pages, https://www.rand.org/pubs/perspectives/PE154.html.

Jennings, W. G., Fridell, L. A., and Lynch, M. D. (2014). Cops and cameras: Officer perceptions of the use of body-worn cameras in law enforcement. *Journal of Criminal Justice*, 42(6):549–556.

Jetelina, K. K., Jennings, W. G., Bishopp, S. A., Piquero, A. R., and Reingle Gonzalez, J. M. (2017). Dissecting the complexities of the relationship between police officer-civilian race/ethnicity dyads and less-than-lethal use of force. *American Journal of Public Health*, 107(7):1164–1170.

Kamruzzaman, M., Kalyanaraman, A., Krishnamoorthy, B., and Schnable, P. (2017). Toward a scalable exploratory framework for complex high-dimensional phenomics data. Submitted; arXiv:1707.04362.

Klinger, D. A. (1995). The micro-structure of nonlethal force: Baseline data from an observational study. *Criminal Justice Review*, 20(2):169–186.

Klinger, D. A. (2012). On the problems and promise of research on lethal police violence: A research note. *Homicide Studies*, 16(1):78–96.

Klinger, D. A. and Brunson, R. K. (2009). Police officers' perceptual distortions during lethal force situations: Informing the reasonableness standard. *Criminology & Public Policy*, 8(1):117–140.

Li, L., Cheng, W.-Y., Glicksberg, B. S., Gottesman, O., Tamler, R., Chen, R., Bottinger, E. P., and Dudley, J. T. (2015). Identification of type 2 diabetes subgroups through topological analysis of patient similarity. *Science Translational Medicine*, 7(311):311ra174–311ra174.

Lum, P. Y., Singh, G., Lehman, A., Ishkanov, T., Vejdemo-Johansson, M., Alagappan, M., Carlsson, J. G., and Carlsson, G. (2013). Extracting insights from the shape of complex data using topology. *Scientific Reports*, 3(1236).

Macnamara, J. R. (2005). Media content analysis: Its uses, benefits and best practice methodology. *Asia Pacific Public Relations Journal*, 6(1):1–34.

Makin, D. A. (2016). When the watchers are watched: An interpretive phenomenological analysis of body-worn cameras. *Journal of Qualitative Criminal Justice & Criminology*, 4(1):113–151.

Makin, D. A., Willits, D. W., Koslicki, W., Brooks, R., Dietrich, B., and Bailey, R. (2018). Contextual determinants of observed negative emotional states in police-community interactions. *Criminal Justice and Behavior*. Forthcoming.

Mastrofski, S. D., Reisig, M. D., and McCluskey, J. D. (2002). Police disrespect toward the public: An encounter-based analysis. *Criminology*, 40(3):519–552.

McCluskey, J. D., Terrill, W., and Paoline, III, E. A. (2005). Peer group aggressiveness and the use of coercion in police-suspect encounters. *Police Practice and Research*, 6(1):19–37.

Morabito, M. S., Kerr, A. N., Watson, A., Draine, J., Ottati, V., and Angell, B. (2012). Crisis intervention teams and people with mental illness: Exploring the factors that influence the use of force. *Crime & Delinquency*, 58(1):57–77.

Morabito, M. S. and Socia, K. M. (2015). Is dangerousness a myth? Injuries and police encounters with people with mental illnesses. *Criminology & Public Policy*, 14(2):253–276.

Munkres, J. R. (1984). *Elements of Algebraic Topology*. Addison–Wesley Publishing Company, Menlo Park.

Nicolau, M., Levine, A. J., and Carlsson, G. (2011). Topology based data analysis identifies a subgroup of breast cancers with a unique mutational profile and excellent survival. *Proceedings of the National Academy of Sciences*, 108(17):7265–7270.

Nielson, J. L., Paquette, J., Liu, A. W., Guandique, C. F., Tovar, C. A., Inoue, T., Irvine, K.-A., Gensel, J. C., Kloke, J., Petrossian, T. C., Lum, P. Y., Carlsson, G. E., Manley, G. T., Young, W., Beattie, M. S., Bresnahan, J. C., and Ferguson, A. R. (2015). Topological data analysis for discovery in preclinical spinal cord injury and traumatic brain injury. *Nature Communications*, 6:8581+.

Nowacki, J. S. and Willits, D. (2016). Adoption of body cameras by united states police agencies: an organisational analysis. *Policing and Society*, pages 1–13.

Phillips, S. W. (2018). Eyes are not cameras: The importance of integrating perceptual distortions, misinformation, and false memories into the police body camera debate. *Policing: A Journal of Policy and Practice*, 12(1):91–99.

Ragin, C. C. (2014). *The Comparative Method: Moving Beyond Qualitative and Quantitative Strategies*. University of California Press, first, with a new introduction edition.

Ross, C., Winterhalder, B., and McElreath, R. (2018). Resolution of apparent paradoxes in the race-specific frequency of use-of-force by police. *Palgrave Communications*, 4:61.

Roussell, A., Henne, K., Glover, K. S., and Willits, D. (2017). Impossibility of a âĂIJreverse racismâĂİ effect. *Criminology & Public Policy*.

Rucco, M., Merelli, E., Herman, D., Ramanan, D., Petrossian, T., Falsetti, L., Nitti, C., and Salvi, A. (2015). Using topological data analysis for diagnosis pulmonary embolism. *Journal of Theoretical and Applied Computer Science*, 9:41–55. http://www.jtacs.org/archive/2015/1/5.

Sarikonda, G., Pettus, J., Phatak, S., Sachithanantham, S., Miller, J. F., Wesley, J. D., Cadag, E., Chae, J., Ganesan, L., Mallios, R., Edelman, S., Peters, B., and von Herrath, M. (2014). CD8 T-cell reactivity to islet antigens is unique to type 1 while CD4 T-cell reactivity exists in both type 1 and type 2 diabetes. *Journal of Autoimmunity*, 50(Supplement C):77–82.

Singh, G., Memoli, F., and Carlsson, G. (2007). Topological Methods for the Analysis of High Dimensional Data Sets and 3D Object Recognition. In Botsch, M., Pajarola, R., Chen, B., and Zwicker, M., editors, *Proceedings of the Symposium on Point Based Graphics*, pages 91–100, Prague, Czech Republic. Eurographics Association.

Terrill, W. (2005). Police use of force: a transactional approach. *Justice Quarterly*, 22(1):107–138.

Torres, B. Y., Oliveira, J. H. M., Thomas Tate, A., Rath, P., Cumnock, K., and Schneider, D. S. (2016). Tracking resilience to infections by mapping disease space. *PLoS Biol*, 14(4):1–19.

White, M. D. (2014). *Police Officer Body-Worn Cameras: Assessing the Evidence*. US Department of Justice: National Institute of Corrections.

Wikström, P.-O. H., Oberwittler, D., Treiber, K., and Hardie, B. (2012). *Breaking Rules: The Social and Situational Dynamics of Young People's Urban Crime*. OUP Oxford.

Willits, D. W. and Makin, D. A. (2018). Show me what happened: Analyzing use of force through analysis of body-worn camera footage. *Journal of Research in Crime and Delinquency*, 55(1):51–77.

Wolfe, S. E. and Nix, J. (2016). The alleged "Ferguson Effect" and police willingness to engage in community partnership. *Law and Human Behavior*, 40(1):1–10.

Worden, R. E. and McLean, S. J. (2014). Systematic social observation of the police. The Oxford Handbook of Police and Policing.

Worrall, J. L., Bishopp, S. A., Zinser, S. C., Wheeler, A. P., and Phillips, S. W. (2018). Exploring bias in police shooting decisions with real shoot/don't shoot cases. *Crime & Delinquency*, 64(9):1171–1192.